DETECTION AND ANALYSIS OF THE $5\nu_3$ ABSORPTION BAND IN $HD^{16}O$

A.D. Bykov, V.A. Kapitanov, S.M. Kobtsev, and O.V. Naumenko

Institute of Atmospheric Optics,
Siberian Branch of the Academy of Sciences of the USSR, Tomsk
Received October 20, 1989

We record the absorption spectrum of the $HD^{16}O$ molecule in the visible region near 0.59 μm using an acoustooptical spectrometer based on a dye laser. The two important features of this experiment were that the acoustooptical detectors were located within the laser cavity and that the laser was operated in two-frequency mode; this leads to a substantial increase in spectrometer sensitivity and an improvement in the controllability and stability of the laser. We carried out an assignment of the lines in the spectrum, determined the rotational and vibrational energy levels for the (005) *state, measured the location of the band center, and determined the rotational constants as well as the centrifugal-distortion coefficients.*

Detailed work involving high-resolution spectra of H_2O and the major isotopomers of H_2O is required for the interpretation of atmospheric spectra and calculating the absorption due to minor atmospheric constituents in the atmospheric transparency windows. Since the $HD^{16}O$ molecule is an asymmetric isotopic modification of H_2O, studying the $HD^{16}O$ spectrum will provide additional information for determining the potential function of the water molecule.

Very little work has been done on the rotational-vibrational structure $HD^{16}O$, especially at high energies. Until recently, only data on 14 vibrational states with quantum numbers ν_1, ν_2, and $\nu_3 \le 3$ and energy $E \le 9300$ cm^{-1} were available in the literature (see Bykov, et al.[1] for the references to the literature). The research on the $3\nu_3$ band carried out by Bykov, et al.[1] extended the range of energies studied in $HD^{16}O$ to 10600 cm^{-1}. The present paper contains an analysis of the $HD^{16}O$ absorption at 0.59 μm.

The vibrational frequencies and anharmonicity constants of $HD^{16}O$ were first improved using the available data from the literature, and the band centers lying near 0.59 μm were calculated. The results of the calculation are given in Table I.

Analysis of the results in Table I leads us to select $5\nu_3$ band as the most promising for investigation for two reasons: first, this band should be relatively strong, and second, the band origin for this band falls at the exact center of the spectral range of emission from the rhodamine 6G dye laser suggested for use in the experiment.

High-excitation states in $HD^{16}O$ are difficult to study for two reasons: first, the line absorption coefficients are small, and second, since the production of $HD^{16}O$ involves an isotopic-exchange reaction of the form

$$2H_2O + 2D_2O \rightleftarrows 2HD^{16}O + H_2O + D_2O,$$

we must be able to distinguish between the absorption spectra of H_2O, $HD^{16}O$, and D_2O.

TABLE I.

Absorption band centers in $HD^{16}O$ *near* 0.59 μm.

Upper state	Band center
114	17832
005	16899
421	16684
104	16525
501	16491
203	15962

Experiment. This distinction can effectively be made in spectrometers based on narrow-band lasers ($\Delta\nu \le 0.001$ cm^{-1}) by recording the absorption due to the mixture and the absorption due to a single component simultaneously with a pair of multipath cells or acoustooptical cells.[2] However, such spectrometers have low sensitivity, and the sensitivity is determined by either the optical path length or the laser source power, respectively. The threshold sensitivity of acoustooptical spectrometers can be increased by a factor of 10–100 by placing the acoustooptical detectors inside the laser cavity.[3] This approach was implemented in the acoustooptic spectrometer whose block diagram is shown in Fig. 1. The spectrometer is based on a continuous narrow-band dye laser.[4] The selective elements of the laser include a thin Fabry-Perot etalon (TE) and a birefringent filter (BF). The laser operates in two-frequency mode, with the laser modes differing in frequency by ≃ 1.8 GHz. The characteristics of the selective elements in the laser have been described

0235-6880/90/02 133–08 $02.00

by Bondarev, et al.[3] The exit mirror has a transmission of 0.5%.

The laser line is scanned over a wide range using the following procedure: the smooth scanning cycle involves adjusting the TE and IF synchronously in such a way that the wavelength of the laser emission varies by $\simeq 7$ cm^{-1}, with the frequencies of the laser modes changing in small steps of 150 MHz, which is the dispersion in the laser cavity. In contrast to Kobtsev and Lunin,[4] we do not use a feedback system based on the intensity of the light reflected from the filter to adjust the birefringent filter relative to the thin etalon when tuning the laser emission line. The adjustment of the filter relative to the etalon during the scanning process is carried out by choosing an appropriate ratio for the control signals fed to the electromechanical drives for the BF and TE. At the end of each smooth scan, the experimental data collection system is blocked, and the thin etalon is rapidly returned to its position (within ~ 10 μs), so that the laser emission for the next smooth-scanning cycle will occur at the next transmission peak of the etalon and the beginning of the next scanning cycle will overlap the end of the previous cycle by approximately 0.3 cm^{-1} for convenience in matching up the sections of the spectrum recorded. The data collection system is then unblocked, and the scan through the laser line continues. This method of synchronously adjusting the selecting elements and joining the scans together enables us to simplify the computer program used to control the spectrometer and expand the capabilities of the microcomputer used for real-time control of the spectrometer.

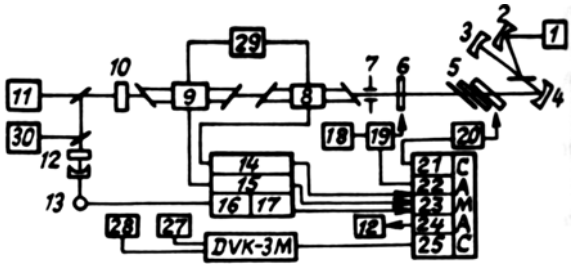

FIG. 1. Block diagram of acoustooptical spectrometer based on an automatic-scanning continuous narrow-band dye laser: 1) argon pump laser; 2) pump mirror; 3) end mirror of due laser; 4) collimator mirror for dye laser; 5) birefringent filter; 6) thin Fabry-Perot etalon; 7) diaphragm; 8) first AOD; 9) second AOD; 10) exit mirror of dye laser; 11) visual monitor for laser spectrum; 12) "marker" (confocal Fabry-Perot interferometer); 13) photodetector; 14, 15) phase-sensitive nanovoltmeters; 16) selective amplifier; 17) synchronoxus detector; 18) audio generator; 19) electromechanical drive for thin etalon; 20) electromechanical drive for birefringent filter; 21) stepper-motor control unit; 22) twelve-bit digital-to-analog converter; 23) ten-bit analog-to-digital converter with switch; 24) plotter driver; 25) K-16 *controller; 26) chart recorder; 27)* 0.5 MB *electronic disk; 28) four-color raster display; 29) vacuum source; 30) wavemeter.*

The following devices were used to monitor the spectral characteristics of the laser: a confocal Fabry-Perot interferometer with dispersion 15 GHz (a so-called "marker interferometer") was used to monitor the smoothness and linearity with which the wavelength of the radiation was varied. The radiation passing through this device then falls on a photodetector whose signal is recorded simultaneously with that from the AODs. The wavelength of the laser radiation at the beginning and end of each smooth scan region was monitored using an IDV-2 wavemeter. A visual laser spectrum monitor[5] is used to obtain real-time information on the spectral composition of the radiation.

The signals from the AODs are detected using a method in which the radiation is frequency-modulated (the spectrometer records the first derivative of the absorption spectrum with respect to frequency). The modulation (frequency 64 Hz and amplitude 0.75 GHz) is introduced using a thin etalon. The amplitude of modulation is chosen from the condition that the signal from the AOD be strongest when the laser line coincides with an absorption line in the material to be studied. The signals from the acoustooptical detectors and the photodetector which records the radiation passing through the marker interferometer are synchronously detected at the modulation frequency using two UNIPAN 232B phase-sensitive nanovoltmeters for each and a laboratory synchronous detector with similar characteristics. A DVK-3M2 computer system and CAMAC are used to further record and process the signals and to control the scanning through the laser emission line.

A ten-bit ADC and switch were used to record the signals after synchronous detection. The resulting first derivatives of the absorption spectra with respect to frequency and the first derivative of the marker interferometer transmission with respect to frequency were plotted in real time on a four-color raster display. At the end of the smooth scanning cycle, the experimental data sets are written in the form of data files on 0.5 MB computer disk. At the end of each smooth scanning cycle, a hard copy plot of the most recent file of experimental data can be obtained using an ENDIM 622.01 plotter/chart recorder driver. The electromechanical drives on the selecting elements are controlled using a 12-bit DAC and the stepper-motor controller described by Butov and Kobtsev.[6] The pump laser is an ILA-120-1 argon laser with an emission power of 2.7 W in all lines.

The spectrometer uses two identical nonresonant AODs with planar condenser microphones and two cells 25 cm in length and 1 cm in diameter. The AODs have a sensitivity on the order of 10–100 V/W · cm^{-1}, which leads to a threshold sensitivity of $< 1 \cdot 10^{-8}$ cm^{-1} for a power of ~ 10 W and an integration time $\tau = 0.3$ s.

In order to separate the absorption spectra of H_2O, $HD^{16}O$, and D_2O, H_2O vapor was placed in one of the AODs and a mixture of $2H_2O + 2D_2O \Leftrightarrow H_2O + 2HD^{16}O$ was placed in the other (Fig. 2). Moreover, since the spectrum of H_2O

In the visible region of the spectrum is fairly well studied[7] and the centers of the absorption lines are known to 0.02–0.005 cm^{-1}, the H_2O absorption lines were used as reference points. The resulting analysis led to the identification of 251 absorption lines as being due to $HD^{1,6}O$.

FIG. 2. Absorption spectra of H_2O *vapor (1) (heavy lines) and a mixture of* H_2O *and* D_2O *vapor (1) (light lines) between* 16 948.002 cm^{-1} *and* 16 943.128 cm^{-1}.

Analysis of the spectrum. The first step in analyzing the spectrum Involved determining the vibrational and rotational constants α_i and β_{ij} of the $HD^{16}O$ molecule from data in the literature. These values were then used to calculate the rotational constants A, B, and C for the states listed in Table I. Using the resulting initial approximation for the (005) vibrational state, we then calculated the absorption spectrum of the $5\nu_3$ band in $HD^{16}O$ and determined the combination differences for the lower state (whose energies were calculated from the spectroscopic constants given by Papineau, et al.[8]) from the strongest lines.

The remainder of the line identification problem involved identifying the desired combination differences. Since most of the error in calculating the transition frequencies involved our relative lack of knowledge concerning the value of the band origin, the search covered a wide range of values around the band origin (± 25 cm^{-1} relative to the initial value) using a specially-developed program. This approach turned out to be quite efficient, and enabled us to quite rapidly determine the band origin of the $5\nu_3$ band (the band origin turned out to be 16 920.024 cm^{-1}, or 21 cm^{-1} higher than the original value) and the energy levels for $J = 1, 2$. Further identifications in the spectrum were carried out in the usual way, in parallel with the solution to the inverse problem. As expected, both type A and type B transitions were present in the spectrum.

Table II gives the basic characteristics of the $HD^{16}O$ absorption spectrum in the region between 16 746 cm^{-1} and 17 012 cm^{-1}. The first column gives the measured line center in inverse centimeters; this is followed by the quantity Δ (equal to the difference between the theoretical and experimental values of the line center), the type of transition, and the theoretical relative line intensities. The final two columns of Table II give the quantum numbers J, K_a, and K_b for the upper and lower levels, respectively. An asterisk after the wavelength indicates that the line in question was not used in solving the inverse problem. The relative intensities were normalized to that of the line at 16 785.745 cm^{-1}, and the intensities of the type B transitions were reduced by an additional factor of ten, which corresponds to the approximate ratio observed in the spectrum.

TABLE II.

Absorption spectrum of $HD^{16}O$ *from* 16 746 cm^{-1} *to* 17 012 cm^{-1}

Line center	$\Delta \cdot 10^3$	Type of transition	Intensity	J'	K'_a	K'_c	J	K_a	K_c
1	2	3	4	5			6		
16746.964	1	A	1.5E-01	7	6	2	7	6	1
16746.964	0	A	1.5E-01	7	6	1	7	6	2
16747.099	-12	A	1.3E-01	5	4	1	6	4	2
16747.099	-16	A	1.3E-01	5	4	2	6	4	3
16748.000	-5	B	1.9E-02	4	2	2	5	3	3
16748.848	9	A	3.5E-01	6	6	1	6	6	0
16748.848	9	A	3.5E-01	6	6	0	6	6	1
16750.129	-7	A	4.0E-01	8	1	7	9	1	8
16761.718*	28	A	4.0E-01	6	3	3	7	3	4
16763.074*	13	A	4.7E-01	7	2	5	8	2	6
16764.405*	41	A	6.4E-02	4	4	0	5	4	1
16764.405*	34	A	6.4E-02	4	4	1	5	4	2
16765.452	-2	A	5.7E-01	7	2	6	8	2	7
16765.676	6	B	5.4-02	8	0	8	9	1	9
16765.776	0	A	7.1E-01	8	1	8	9	1	9
16766.032	0	A	7.1E-01	8	0	8	9	0	9

Line center	$\Delta \cdot 10^3$	Type of transition	Intensity	J′	K'_a	K'_c	J	K_a	K_c
1	2	3	4	5			6		
16766.147	8	B	5.4E-02	8	1	8	9	0	9
16769.313*	29	A	3.6E-05	4	1	4	4	3	1
16771.420*	-30	A	9.2E-04	9	0	9	9	2	8
16771.602	-8	A	6.3E-01	7	1	6	8	1	7
16775.437*	-34	B	2.4E-02	6	1	5	7	2	6
16775.915*	-22	B	3.9E-02	2	2	1	3	3	0
16776.824	-13	B	1.3E-02	7	2	6	8	1	7
16778.956*	17	A	4.2E-01	5	3	3	6	3	4
16781.919	-4	A	6.8E-01	6	2	4	7	2	5
16784.434	-11	A	7.6E-01	6	2	5	7	2	6
16785.060	4	B	7.5E-02	7	0	7	8	1	8
16785.313	8	A	1.0E+00	7	1	7	8	1	8
16785.745	-2	A	1.0E+00	7	0	7	8	0	8
16785.995	-1	B	7.3E-02	7	1	7	8	0	8
16788.767	-4	B	2.6E-02	5	1	4	6	2	5
16789.285	-5	A	9.1E-03	10	5	6	10	5	5
16790.036	0	B	7.8E-03	3	1	3	4	2	2
16790.486*	-29	A	1.7E-03	8	0	8	8	2	7
16791.862	4	A	2.5E-02	9	5	5	9	5	4
16791.979	-1	A	9.0E-01	6	1	5	7	1	6
16792.682	6	A	2.5E-02	9	5	4	9	5	5
16793.255	-13	A	2.9E-03	7	1	6	7	3	5
16794.364	8	A	6.6E-02	8	5	3	8	5	4
16796.142	20	A	3.4E-01	4	3	1	5	3	2
16796.227	-5	A	1.6E-01	7	5	2	7	5	3
16796.332	9	A	3.4E-01	4	3	2	5	3	3
16798.088	6	A	3.7E-01	6	5	5	6	5	1
16798.088	-4	A	3.7E-01	6	5	1	6	5	2
16799.070	-4	A	2.5E-04	4	1	3	4	3	2
16799.817	2	A	8.4E-01	5	5	1	5	5	0
16799.817	1	A	8.4E-01	5	5	0	5	5	1
16800.015	12	A	8.4E-01	5	2	3	6	2	4
16800.933	9	B	2.7E-02	4	1	3	5	2	4
16802.606*	-17	A	8.8E-01	5	2	4	6	2	5
16803.460	-13	B	9.4E-02	6	0	6	7	1	7
16804.035	-2	A	1.3E+00	6	1	6	7	1	7
16804.760	2	A	1.3E+00	6	0	6	7	0	7
16805.323	0	B	8.9E-02	6	1	6	7	0	7
16811.139	0	A	1.1E+00	5	1	4	6	1	5
16812.863	-2	B	2.7E-02	3	1	2	4	2	3
16813.260	-4	A	1.5E-01	3	3	0	4	3	1
16814.561	5	B	1.4E-02	2	1	2	3	2	1
16817.673	-3	A	8.6E-01	4	2	2	5	2	3
16820.130	13	A	8.6E-01	4	2	3	5	2	4
16820.752	11	B	1.0E-01	5	0	5	6	1	6
16821.968	4	A	1.5E+00	5	1	5	6	1	6
16823.043	2	A	1.5E+00	5	0	5	6	0	6
16823.683	-11	A	6.1E-03	10	4	7	10	4	6
16824.275	10	B	9.4E-02	5	1	5	6	0	6
16824.603	8	A	2.8E-03	7	1	7	7	1	6
16824.603	2	A	4.5E-03	9	7	3	8	7	2
16824.603	1	A	4.5E-03	9	7	2	8	7	1
16825.001	10	B	1.0E-02	5	2	4	6	1	5
16825.300	0	B	2.7E-02	2	1	1	3	2	2
16825.994	1	B	1.4E-02	4	2	2	4	3	1
16829.319	-6	A	1.2E+00	4	1	3	5	1	4
16833.934	-3	A	4.8E-02	8	4	5	8	4	4

Line center	$\Delta \cdot 10^3$	Type of transition	Intensity	J′	K'_a	K'_c	J	K_a	K_c
1	2	3	4	5			6		
16833.934	-3	A	4.8E-02	8	4	5	8	4	4
16835.190	0	A	6.5E-01	3	2	1	4	2	2
16835.544*	-26	A	5.0E-03	8	2	7	8	2	6
16835.708	-12	A	5.1E-03	5	0	5	5	2	4
16836.606*	-20	B	1.0E-01	4	0	4	5	1	5
16836.788	-3	A	1.2E-01	7	4	4	7	4	3
16837.070	2	A	6.4E-01	3	2	2	4	2	3
16838.232	-7	A	4.4E-02	8	4	4	8	4	5
16838.328	-12	A	1.1E-02	7	4	3	7	4	4
16838.952	-6	A	2.9E-01	6	4	3	6	4	2
16839.094	-3	A	1.5E+00	4	1	4	5	1	5
16839.395	-7	A	2.8E-01	6	4	2	6	4	3
16840.540	-5	A	1.6E+00	4	0	4	5	0	5
16840.741	-5	A	6.6E-01	5	4	2	5	4	1
16840.827	-11	A	6.6E-01	5	4	1	5	4	2
16842.255*	-28	A	1.4E+00	4	4	1	4	4	0
16842.255*	-38	A	1.4E+00	4	4	0	4	4	1
16846.920	-3	A	1.1E+00	3	1	2	4	1	3
16850.985*	-18	B	8.2E-02	3	0	3	4	1	4
16851.992	-5	A	1.8E-03	3	0	3	3	2	2
16852.539	1	A	2.7E-01	2	2	0	3	2	1
16853.346*	14	A	2.0E-02	8	3	6	8	3	5
16853.595	-4	A	2.7E-01	2	2	1	3	2	2
16855.285	8	A	1.2E-02	7	2	6	7	2	5
16855.285*	-14	A	9.9E-03	7	6	2	6	6	1
16855.285*	-15	A	9.9E-03	7	6	1	6	6	0
16855.493	3	A	1.3E+00	3	1	3	4	1	4
16857.222	-7	A	1.5E+00	3	0	3	4	0	4
16861.680	-36	B	5.6E-02	3	1	3	4	0	4
16862.495*	23	A	5.6E-02	7	3	5	7	3	4
16864.227	-1	A	8.3E-01	2	1	1	3	1	2
16865.349	6	A	9.4E-03	5	1	5	5	1	4
16868.789	3	A	2.0E-02	8	6	3	7	6	2
16868.789	-4	A	2.0E-02	8	6	2	7	6	1
16871.231	1	A	9.0E-01	2	1	2	3	1	3
16872.044	1	A	3.3E-01	5	3	3	5	3	2
16873.243	9	A	1.1E+00	2	0	2	3	0	3
16874.317	6	A	7.8E-01	4	3	2	4	3	1
16874.858	14	A	3.2E-01	5	3	2	5	3	3
16875.815	4	A	1.8E-00	3	3	1	3	3	0
16875.922	4	A	1.8E+00	3	3	0	3	3	1
16876.127	-10	A	1.2E-01	6	3	3	6	3	4
16879.595*	-14	A	4.3E-02	7	3	4	7	3	5
16880.280	-11	B	2.7E-02	2	1	2	3	0	3
16881.397	13	A	3.4E-01	1	1	0	2	1	1
16881.996	12	A	1.8E-02	4	1	4	4	1	3
16882.181*	26	A	2.2E-02	9	6	4	8	6	3
16882.181	-6	A	2.2E-02	9	6	3	8	6	2
16883.503	0	A	8.0E-02	5	2	4	5	2	3
16885.381	8	A	1.4E-02	8	3	5	8	3	6
16886.415	-2	A	3.5E-01	1	1	1	2	1	2
16887.424	1	A	1.8E-03	10	2	8	9	4	5
16888.909	2	A	6.6E-01	1	0	1	2	0	2
16891.284	4	A	3.4E-02	6	5	2	5	5	1
16891.284	-4	A	3.4E-02	6	5	1	5	5	0

Line center	$\Delta \cdot 10^3$	Type of transition	Intensity	J'	K'_a	K'_c	J	K_a	K_c
1	2	3	4	5			6		
16891.284	-4	A	3.4E-02	6	5	1	5	5	0
16891.936	19	A	2.0E-01	4	2	3	4	2	2
16895.421	10	A	4.1E-02	3	1	3	3	1	2
16895.562	2	A	1.8E-02	10	6	4	9	6	3
16897.042	-4	A	5.0E-01	3	2	2	3	2	1
16898.114	-3	A	1.5E-04	3	0	3	2	2	0
16898.373	-6	B	6.9E-02	2	0	2	2	1	1
16899.700*	-19	A	1.3E+00	2	2	1	2	2	0
16900.494	-15	A	3.7E-03	7	1	6	6	3	3
16900.672	-4	A	1.3E+00	2	2	0	2	2	1
16901.464	3	A	1.4E-03	10	3	7	10	3	8
16901.632	-5	A	4.7E-01	3	2	1	3	2	2
16901.632	-5	A	4.7E-01	3	2	1	3	2	2
16904.515	-2	A	1.9E-01	0	0	0	1	0	1
16904.628	-1	A	1.7E-01	4	2	2	4	2	3
16905.025	6	A	7.4E-02	7	5	3	6	5	2
16905.069	10	A	7.4E-02	7	5	2	6	5	1
16905.430	-6	A	1.0E-01	2	1	2	2	1	1
16907.531	11	A	1.9E-03	5	0	5	4	2	2
169[illegible]	[illegible]	A	[illegible]	[illegible]			[illegible]		
16912.043	-4	A	4.0E-01	1	1	1	1	1	0
16917.175	4	A	2.6E-02	6	2	4	6	2	5
16917.752	-8	A	4.0E-01	1	1	0	1	1	1
16918.888	14	A	8.6E-02	8	5	3	7	5	2
16922.522	-10	A	1.0E-01	2	1	1	2	1	2
16925.695*	-27	A	1.0E-02	7	2	5	7	2	6
16929.523	7	A	4.4E-02	3	1	2	3	1	3
16932.063	2	B	4.3E-02	1	1	0	1	0	1
16932.225	13	A	7.5E-02	9	5	5	8	5	4
16932.689	3	A	2.1E-01	6	4	3	5	4	2
16932.899	0	A	7.4E-02	9	5	4	8	5	3
16933.038	4	A	2.1E-01	6	4	2	5	4	1
16934.516	0	B	8.7E-02	2	1	1	2	0	2
16935.064	-15	A	2.1E-01	1	0	1	0	0	0
16936.963	-2	A	2.0E-01	4	3	2	3	3	1
16937.474	-7	A	2.0E-01	4	3	1	3	3	0
16938.178	0	A	2.1E-02	4	1	3	4	1	4
16939.540	0	B	1.3E-01	6	2	4	6	1	5
16940.098	-4	B	7.7E-02	6	3	3	6	2	4
16940.565	0	B	7.4E-02	3	2	1	3	1	2
16941.738*	28	B	1.6E-02	8	4	5	8	3	6
16941.810	-2	A	4.0E-01	2	1	2	1	1	1
16945.179	-5	A	3.4E-01	3	2	2	2	2	1
16945.595	0	A	5.3E-02	10	5	6	9	5	5
16946.530	19	A	2.7E-01	7	4	4	6	4	3
16947.700	6	A	2.6E-01	7	4	3	6	4	2
16947.759	2	A	3.3E-01	3	2	1	2	2	0
16948.[illegible]	[illegible]	A	4.0E-01	2	1	1	1	1	0
16948.688	-8	B	3.2E-02	4	3	1	4	2	2
16949.052	-3	A	7.6E-01	2	0	2	1	0	1
16950.238	4	B	2.3E-02	9	2	7	9	1	8
16950.966	0	A	4.9E-01	5	3	3	4	3	2
16952.853*	21	A	4.8E-01	5	3	2	4	3	1
16953.179	2	B	3.6E-02	6	3	4	6	2	5
16953.752	7	A	1.1E+00	3	1	3	2	1	2
16956.127*	14	B	4.3E-02	2	1	2	1	0	1
16957.304*	22	A	6.4E-03	6	1	5	6	1	6

Line center	$\Delta \cdot 10^3$	Type of transition	Intensity	J'	K'_a	K'_c	J	K_a	K_c
1	2	3	4	5			6		
16957.404*	33	B	3.0E-02	4	2	3	4	1	4
16958.370	6	A	8.7E-01	4	2	3	3	2	2
16958.602*	-44	A	3.2E-02	11	5	7	10	5	6
16959.573	-10	B	3.6E-02	6	1	5	6	0	6
16960.022	16	A	2.5E-01	8	4	5	7	4	4
16961.213	0	A	1.4E+00	3	0	3	2	0	2
16961.601*	-32	B	2.8E-02	5	2	4	5	1	5
16963.626*	29	A	1.4E-03	4	2	3	4	0	4
16963.725	3	A	1.0E+00	3	1	2	2	1	1
16964.397	10	A	6.6E-01	6	3	4	5	3	3
16964.582	11	A	1.7E+00	4	1	4	3	1	3
16965.549	-3	A	2.4E-03	5	2	4	5	0	5
16966.995	-16	B	2.0E-02	7	1	6	7	0	7
16969.237	-4	A	6.1E-01	6	3	3	5	3	2
16970.460	4	A	1.2E+00	5	2	4	4	2	3
16971.172	11	A	1.9E+00	4	0	4	3	0	3
16972.911	0	A	1.9E-01	9	4	6	8	4	5
16974.200	3	A	2.1E+00	5	1	5	4	1	4
16976.142	-1	A	1.6E-03	8	2	7	8	0	8
16976.490	-2	B	3.0E-02	2	2	1	1	1	0
16978.105	5	A	1.6E+00	4	1	3	3	1	2
16979.210	10	A	2.1E+00	5	0	5	4	0	4
16979.792	-2	B	3.0E-02	2	0	2	1	1	1
16981.720	4	A	1.1E+00	5	2	3	4	2	2
16982.635	16	A	2.2E+00	6	1	6	5	1	5
16985.970	-3	A	2.2E+00	6	0	6	5	0	5
16986.860	10	A	5.8E-01	7	3	4	6	3	3
16987.925	-1	B	4.2E-02	3	2	2	2	1	1
16988.220	-2	A	5.5E-01	8	3	6	7	3	5
16989.912	15	A	2.0E+00	7	1	7	6	1	6
16990.531	6	A	1.2E+00	7	2	6	6	2	5
16990.671	8	A	1.8E+00	5	1	4	4	1	3
16991.964	15	A	2.0E+00	7	0	7	6	0	6
16995.429	-14	B	3.7E-02	8	1	7	7	2	6
16996.016	0	B	1.3E-01	8	0	8	7	1	7
16996.114	-8	A	1.7E+00	8	1	8	7	1	7
16997.312	12	A	1.6E+00	8	0	8	7	0	7
16997.397	-9	B	1.3E-01	8	1	8	7	0	7
16998.003	17	A	3.9E-01	9	3	7	8	3	6
16998.042	8	A	1.2E+00	6	2	4	5	2	3
16998.230	-1	A	9.9E-01	8	2	7	7	2	6
17000.664	2	A	1.6E+00	6	1	5	5	1	4
17001.338	3	A	1.2E+00	9	1	9	8	1	8
17002.023	-8	A	1.2E+00	9	0	9	8	0	8
17005.018	-13	A	4.6E-01	8	3	5	7	3	4
17005.660	-1	B	3.0E-02	6	6	1	5	5	0
17005.660	-1	B	3.0E-02	6	6	0	5	5	1
17005.797*	33	A	8.7E-01	10	1	10	9	1	9
17006.170*	44	B	7.2E-02	10	1	10	9	0	9
17007.641*	-24	A	1.3E+00	7	1	6	6	1	5
17009.319	0	A	5.5E-01	11	1	11	10	1	10
17010.851	-2	A	1.9E-03	3	2	1	2	0	2
17011.936	-17	A	9.7E-01	8	1	7	7	1	6

As a result, only 29 of the 251 $HD^{16}O$ lines found in the spectrum remained unidentified. All of the identified lines were assigned to the $5\nu_3$ band, and no lines from other bands were observed.

In analyzing the spectra, we determined 86 energy levels with $J \le 11$ and $K_a \le 7$ in the (005) state of $HD^{16}O$. These results are given in Table III; the rms errors in the energy levels and the differences Δ between the theoretical and experimental values are given in parentheses. Each energy level was generally determined from two to three lines. When no rms error is given in Table III, this indicates that the level was determined from a single line center. These are mostly energy levels corresponding to large values of the quantum numbers J and K_a.

Asymmetric isotopic substitution has a strong effect on the relationship between the three normal frequencies in the water molecule. In the water molecule, $\omega_1 \approx 2\omega_2 \approx \omega_3$, and this leads to the well-known Coriolis, Fermi, and Darling-Dennison resonances between states of the form $\nu_1\nu_2\nu_3$ and states of the form $\nu_1\pm1\ \nu_2\nu_3\mp1$, $\nu_1\nu_2\pm2$, $\nu_3\mp1$, $\nu_1\pm2$, $\nu_2\nu_3\mp2$, and $\nu_1\pm1$, $\nu_2\mp2\nu_3$. This means that the vibrational states in H_2O form polyads of states linked by resonant interactions. For example, the lines in the 0.59 μm absorption band are due to transitions belonging to a polyad of 21 vibrational levels. In the $HD^{16}O$ molecule, we have only one approximate relation, $\omega_1 \approx 2\omega_{2r}$. which leads to resonances between states of the form $\nu_1\nu_2\nu_3$ and states of the form $\nu_1\pm1\ \nu_2\pm2\nu_3$. In this case, states of the form (0 0 ν) can be treated as isolated, at least for small J.

TABLE III.

Energy levels in the (005) *state of* $HD^{16}O$ (cm^{-1}).

J	K_a	K_c	E_{exp}	$\Delta\cdot10^3$	J	K_a	K_c	E_{exp}	$\Delta\cdot10^3$
	1		2	3		4		5	6
0	0	0	16920.023	2	6	5	1	17507.254 (1)	4
1	0	1	16935.073 (13)	7	6	6	1	17621.634 (7)	-4
1	1	1	16944.542 (4)	2	6	6	0	17621.634 (7)	33
1	1	0	16947.571 (10)	-2	7	0	7	17298.268 (9)	-5
2	0	2	16964.563 (8)	0	7	1	7	17298.519 (7)	-7
2	1	2	16971.620 (4)	1	7	1	6	17370.159 (3)	13
2	1	1	16980.691 (4)	-2	7	2	6	17375.397 (1)	3
2	2	1	17008.985 (1)	3	7	3	4	17456.523	-10
2	2	0	17009.600 (2)	3	7	4	4	17520.408 (16)	-7
3	0	3	17007 382 (3)	3	7	4	3	17521.658 (10)	6
3	1	3	17011.877 (4)	-5	7	5	3	17614.191	-6
3	1	2	17029.907 (5)	0	7	5	2	17614.235 (40)	3
3	2	2	17054.108 (3)	2	7	6	2	17728.092	0
3	2	1	17057.025 (3)	0	7	6	1	17028.092	0
3	3	1	17108.866	-4	8	0	8	17400.465 (6)	-4
3	3	0	17108.941 (6)	0	8	1	8	17400.564 (7)	3
4	0	4	17062.494 (12)	-3	8	1	7	17485.857 (5)	13
4	1	4	17064.965 (11)	-3	8	2	7	17488.657 (1)	2
4	1	3	17094.561 (6)	0	8	3	6	17565.124	3
4	2	3	17113.763 (5)	10	8	3	5	17586.990 (15)	3
4	2	2	17121.669 (2)	2	8	4	5	17643.335 (13)	-6
4	3	2	17169.992 (6)	-4	8	4	4	17646.794	7
4	3	1	17170.533 (15)	0	8	5	3	17736.897 (4)	-10
5	0	5	17129.364 (5)	-8	8	6	3	17849.917	-2
5	1	5	17130.583 (1)	-4	8	6	2	17849.917	4
5	1	4	17173.647 (5)	0	9	0	9	17514.538	9
5	2	4	17187.500 (6)	-2	9	1	9	17514.594	-2
5	2	3	17203.558 (4)	-6	9	2	7	17685.972	-4
5	3	2	17248.523	-13	9	4	6	17781.473	0
5	4	2	17320.994 (7)	11	9	5	5	178.74751 (6)	-8
5	4	1	17321.069 (1)	12	9	5	4	17875.463 (4)	-4
5	5	1	17415.786	-2	9	7	3	18119.438	0
5	5	0	17415.786	0	9	7	2	18119.438	0
6	0	6	17207.914 (8)	5	10	2	8	17839.058	0
6	1	6	17208.482 (3)	1	10	3	8	17847.346	-5
6	1	5	17265.894 (6)	4	10	3	7	17897.256	-3
6	2	5	17274.861	11	10	4	7	17934.441	11
6	2	4	17302.046 (4)	0	10	5	6	18028.375 (4)	4
6	3	4	17338.058 (7)	-5	10	6	4	18140.000	0
6	3	3	17343.644 (3)	7	11	0	11	17778.435	-7
6	4	3	17412.926 (6)	2	11	1	11	17778.435	0
6	4	2	17413.290 (8)	3					
6	5	2	17507.254 (1)	-5					

We therefore used the Watson Hamiltonian to solve the Inverse problem of determining the rotational and centrifugal-distortion constants:

$$H = E + \left(A - \frac{B+C}{2}\right)J_z^2 + \frac{B+C}{2}J^2 - \Delta_K J_z^4 - \Delta_{JK} J_z^2 J^2 - \Delta_J J^4 + H_K J_z^6 + H_{KJ} J_z^4 J^2 + H_{JK} J_z^2 J^4 + H_J J^6 + L_K J_z^8 + P_K J_z^{10} + \frac{B-C}{2} J_{xy}^2 - \delta_K \{J_z^2, J_{xy}^2\} - 2\delta_J J^2 J_{xy}^2 + h_K \{J^4, J_{xy}^2\}, \quad (1)$$

where J_x, J_y, and J_z are the angular-momentum operators, $J_{xy}^2 = J_x^2 - J_y^2$, $\{AB\} = AB + BA$.

TABLE IV.

Spectroscopic constants of the (005) *state in* $HD^{16}O$ (cm^{-1}).

Parameter	Value	Parameter	Value
E	16920.0248_6 (23)	$\delta_J\cdot10^4$	1.5064_6 (76)
A	18.51317_9 (72)	$H_K\cdot10^5$	2.59_0 (15)
B	9.04438_9 (22)	$H_{KJ}\cdot10^6$	-9.269
C	6.01198_5 (22)	$H_{JK}\cdot10^6$	3.143_8 (85)
$\Delta_K\cdot10^3$	8.165_9 (63)	$H\cdot10^7$	1.63_0 (20)
$\Delta_{JK}\cdot10^5$	3.7_9 (12)	$h_K\cdot10^5$	1.981_6 (45)
$\Delta_J\cdot10^4$	4.324_5 (36)	$L_K\cdot10^7$	-2.512
$\delta_K\cdot10^3$	1.531_8 (11)	$P_K\cdot10^9$	3.45_3 (21)

Table IV gives spectroscopic constants determined for the (005) state of $HD^{16}O$ and the 68%

confidence intervals for these values in units of the last significant figures. Two parameters (H_{KJ} and L_K) were not varied, but assumed to be equal to their for the ground vibrational state.

The set of parameters obtained above reproduces the experimental energy levels to within a rms error of $6 \cdot 10^{-3}$cm^{-1}. The percentage distribution of energy levels with respect to the deviation between the experimental values and the theoretical values is as follows:

$0 < \delta \le 5 \cdot 10^{-3}$ cm^{-1} 72% of the levels

$5 \cdot 10^{-3} < \delta \le 1 \cdot 10^{-2}$ cm^{-1} 19%,

$1 \cdot 10^{-2} < \delta \le 1.8 \cdot 10^{-2}$ cm^{-1} 9%,

where $\delta = \left|E_{\exp} - E_{th}\right|$. Thus. 91% of all the levels are described to within 0.01 cm^{-1}.

The rotational constants A, B, and C obtained by solving the inverse problem (18.513, 9.044, and 6.011 cm^{-1}, respectively) turned out to be quite close to the initial values of the rotational constants (18.595, 8.980, and 6.013 cm^{-1}), which confirms that the selected model is correct and that we have interpreted the band correctly.

We note in conclusion that the unique high-sensitivity, high-spectral-resolution spectrometer developed for visible wavelengths here will make it possible to carry out precision measurements of absorption spectra, and the spectroscopic parameters obtained for the high-excitation (005) state will improve our knowledge of the structure of the energy levels in this molecule and enable us to carry out better calculations of a predictive nature.

REFERENCES

1. A.D. Bykov, T.M. Kadoshnikova, C.E. Sabinina, V.I. Serdjukov, and L.N. Sinitsa, Atmos. Opt. **2**, No. 9. 770–773 (1989).
2. V.E. Zuev and Yu.N. Ponomarev, Zh. Prikl. Spectrosk. **45**, No. 1, 52–56 (1986).
3. B.V. Bondarev,V.A. Kapitanov, S.M. Kobtsev, and Yu.N. Ponomarev, Opt. Atmos. **1**, No. 10, 18–25 (1988).
4. S.M. Kobtsev and V.M. Lunin, Prib. Tekh. Eksp. No. 1. 240–241 (1989).
5. B.V. Bondarev, A.V. Korablev, S.M. Kobtsev, and V.T. Makashev, Prib. Tekh. Eksp. No. 5, 185–189 (1989).
6. I.V. Butov and S.M. Kobtsev, Prib. Tekh. Eksp., No. 1. 243–246 (1989).
7. C. Camy-Peyret, J.M. Flaud, J.P. Chevillard, et al., J. Mol. Spectrosc. **113**, 208–228 (1985).
8. N. Papineau, C. Camy-Peyret, J.M. Flaud, and G. Guelachvili, J. Mol. Spectrosc. **92**, 451–468 (1982).